JACS
JOURNAL OF THE AMERICAN CHEMICAL SOCIETY

COMMUNICATION

pubs.acs.org/JACS

A More Reactive Trigonal-Bipyramidal High-Spin Oxoiron(IV) Complex with a cis-Labile Site

Jason England,[†] Yisong Guo,[‡] Katherine M. Van Heuvelen,[†] Matthew A. Cranswick,[†] Gregory T. Rohde,[†] Emile L. Bominaar,*[,‡] Eckard Münck,*[,‡] and Lawrence Que, Jr.*[,†]

[†]Department of Chemistry and Center for Metals in Biocatalysis, University of Minnesota, Minneapolis, Minnesota 55455, United States

[‡]Department of Chemistry, Carnegie Mellon University, Pittsburgh, Pennsylvania 15213, United States

Supporting Information

ABSTRACT: The trigonal-bipyramidal high-spin (S = 2) oxoiron(IV) complex $[Fe^{IV}(O)(TMG_2dien)(CH_3CN)]^{2+}$ (**7**) was synthesized and spectroscopically characterized. Substitution of the CH_3CN ligand by anions, demonstrated here for X = N_3^- and Cl^-, yielded additional S = 2 oxoiron(IV) complexes of general formulation $[Fe^{IV}(O)(TMG_2dien)(X)]^+$ (**7-X**). The reduced steric bulk of **7** relative to the published S = 2 complex $[Fe^{IV}(O)(TMG_3tren)]^{2+}$ (**2**) was reflected by enhanced rates of intermolecular substrate oxidation.

Non-heme monoiron oxygen-activating enzymes perform a remarkably diverse array of highly selective oxidative transformations.[1] Most have iron centers with a 2-His-1-carboxylate facial triad structural motif, and their catalytic cycles often involve oxoiron(IV) intermediates as oxidants. Within the past several years, such oxoiron(IV) species have been trapped and spectroscopically characterized in several enzymes and found in all cases to be high-spin (S = 2).[2] In contrast, the overwhelming majority of existing synthetic oxoiron(IV) complexes have S = 1 ground states.[3] To date, the only published examples of S = 2 oxoiron(IV) complexes are $[Fe^{IV}(O)(H_2O)_5]^{2+}$ (**1**),[4] $[Fe^{IV}(O)(TMG_3tren)]^{2+}$ (**2**; TMG_3tren =1,1,1-tris{2-[N^2-(1,1,3,3-tetramethylguanidino)]ethyl}amine),[5] and $[Fe^{IV}(O)(H_3buea)]^-$ (**3**; H_3buea = tris[(N'-*tert*-butylureaylato)-*N*-ethylene]amine trianion).[6] The crystallographically characterized trigonal-bipyramidal (TBP) complex **2** was found to react rapidly via intramolecular ligand hydroxylation ($t_{1/2}$ at 25 °C = 30 s) but reacted with external hydrocarbon substrates at rates comparable to those of existing S = 1 complexes. In view of the fact that many density functional theory (DFT) studies have predicted more facile H-atom abstraction by S = 2 oxoiron(IV) centers than by their S = 1 counterparts,[7] the intermolecular reactivity observed for **2** was disappointingly sluggish, a fact attributed to steric retardation of the reaction due to the bulk of the tetramethylguanidine donors.[5a,8] In an effort to assess and rationalize the inherent reactivity of the S = 2 oxoiron(IV) center in **2**, we sought to (i) reduce the steric bulk of the supporting ligand and (ii) expand the palette of existing high-spin oxoiron(IV) complexes. Both aims were easily accommodated by replacement of one arm of the tripodal TMG_3tren ligand with a methyl group to yield the tridentate TMG_2dien ligand (Figure 1A).

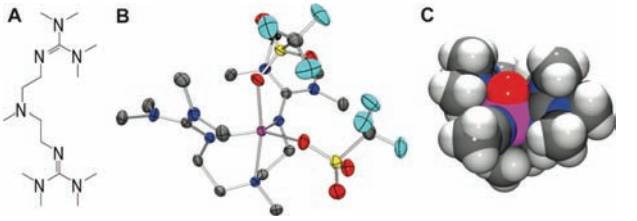

Figure 1. (A) Structure of the TMG_2dien ligand. (B) Thermal ellipsoid plot of $[Fe^{II}(TMG_2dien)(OTf)_2]$ (**4**) showing 50% probability ellipsoids. Hydrogen atoms have been omitted for clarity. Selected bond distances (Å): $Fe-O_{axial}$, 2.2012(15); $Fe-O_{equatorial}$, 2.0816(15); $Fe-N_{axial}$, 2.2835(17); $Fe-N_{guanidine}$(av), 2.0597(17). (C) Space-filling model of the DFT-generated structure of **7**. Atom color scheme: C, gray; F, light-blue; Fe, magenta; H, white; N, blue; O, red; S, yellow.

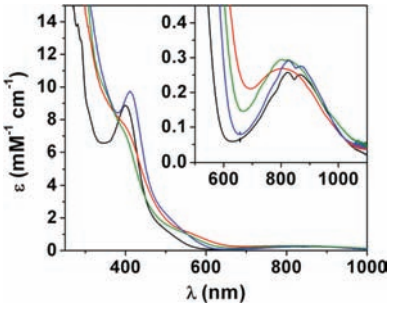

Figure 2. Electronic spectra of **2** (black line), **7** (red line), **7-N$_3$** (blue line), and **7-Cl** (green line) in CH_3CN solution. Inset: expansion of the features in the NIR region.

The iron(II) starting material used in this study, $[Fe^{II}(TMG_2dien)(OTf)_2]$ (**4**), was prepared by thallium(I) salt metathesis of the chloride ligands in $[Fe^{II}(TMG_2dien)(Cl)_2]$ (**5**), which itself was generated by combining equimolar quantities of TMG_2dien and $FeCl_2$. The high-resolution X-ray structures of **4** [Figure 1B and Table S1 in the Supporting Information (SI)] and **5** (Figure S1 and Table S2) revealed five-coordinate complexes with geometries intermediate between square-pyramidal (SP) and TBP (τ = 0.64 and 0.56, respectively).[9] This contrasts with the strictly TBP geometry of

Received: May 3, 2011
Published: July 08, 2011

Table 1. Spectroscopic Parameters of Selected $S = 2$ Oxoiron(IV) Complexes

complex	λ_{max} [nm] (ε_{max} [M^{-1} cm^{-1}])	$\nu_{Fe=O}$ ($\Delta^{18}O$) [cm^{-1}]	D [cm^{-1}]	E/D	$A_{x,y,z}/g_n\beta_n$ [T]	ΔE_Q [mm s^{-1}]	η	δ [mm s^{-1}]	E_0 [eV]	E_{PE} [eV] (area)
7	380 (8200),[a] 805 (270)	807 (−34)	4.5,[b] 4.2[c]	0.09,[b] 0.10[c]	−13.9, −15.8, −26.0	0.58[d]	0.5	0.08	7123.6	7113.3 (19.9), 7115.0 (3.1)
7-N$_3$	412 (9700), 827 (290), 867 (275)	833 (−38)	4.6,[b] 5.0[c]	0.04,[b] 0.05[c]	−15.5, −14.5, −27.0	−0.30[e]	0.35	0.12	7124.2	7113.8 (24.7), 7115.7 (9.2), 7118.1 (5.5)
7-Cl	385 (7800),[a] 803 (295), 825 (293)	810 (−35)	4.1,[b] 4.2[c]	0.13,[b] 0.14[c]	−15.1, −15.4, −26.6	0.41	0.53	0.08	7123.9	7113.9 (21.9), 7115.7 (2.1)
2[f]	400 (8900), 825 (260), 865 (250)	843	5.0	0.02	−15.5, −14.8, −28.0	−0.29	0	0.09	7123.2	7113.8 (23.9), 7115.6 (3.1)
3[g]	350 (4200), 440 (3100), 550 (1900), 808 (280)	798	4.0	0.03	–	0.43	–	0.02	–	–
1[h]	320	–	9.7	0	−20.3, −20.3, nd	−0.33	0	0.38	7126	7114.5 (60−70)
TauD-J[i]	318	821	10.5	0.01	−18.4, −17.6, −31.0	−0.9	0	0.30	7123.8[j]	–

[a] Shoulder. [b] Determined by Mössbauer spectroscopy. [c] Determined by EPR spectroscopy. [d] The electric-field gradient (EFG) tensor and the **A** tensor were rotated relative to the ZFS tensor by $\alpha_{EFG} = 50°$, $\beta_{EFG} = 45°$ and $\alpha_A = 55°$, respectively (WMOSS convention); see the SI for comments. [e] The EFG tensor and the **A** tensor were rotated by $\alpha_{EFG} = 30°$, $\beta_{EFG} = 60°$ and $\alpha_A = 20°$, respectively. [f] Reference 5a. [g] Reference 6. [h] Reference 4. [i] Data were taken from refs 2b and 14. [j] Assuming an Fe foil reference E of 7112.0 eV.

[Fe^{II}(TMG$_3$tren)(OTf)](OTf) (**6**; $\tau = 0.96$), the iron(II) starting material used in the generation of **2**.[5a]

Treatment of a CH_3CN solution of **4** with 2-(*tert*-butylsulfonyl)iodosylbenzene, 2-(^{t}BuSO$_2$)C$_6$H$_4$IO,[10] yielded the orange-brown species **7** ($t_{1/2}$ at −30 °C ≈ 0.5 h vs 4.5 h for **2**), whose electronic spectrum is reminiscent of that for **2** (Figure 2 and Table 1), with a weak near-IR (NIR) band centered at 805 nm (ε = 270 M^{-1} cm^{-1}) and an intense UV absorption having a shoulder at ca. 380 nm (ε = 8200 M^{-1} cm^{-1}). Notably, maximization of the intensity of the aforementioned NIR band required the addition of 2.5−3 equiv of oxidant. Mössbauer spectroscopy revealed that reaction with 1 equiv of oxidant led to substoichiometric yields of **7** (45%), with the remainder of the iron content being associated primarily with unreacted **4** (Figure S2). The absence of other iron products is consistent with nonproductive reaction of 2-(^{t}BuSO$_2$)C$_6$H$_4$IO due to metal-catalyzed disproportionation, a process that has been documented for this oxidant.[10] Additionally, the ^{19}F NMR spectrum of **7** in CD_3CN displayed a *single* peak at −80 ppm, which is indicative of free triflate, suggesting that the potentially cis-labile site is filled by a solvent ligand. This observation, combined with the other data detailed herein, led to the formulation of **7** as [Fe^{IV}(O)(TMG$_2$dien)(CH_3CN)]$^{2+}$.

One of the primary motivations for developing the chemistry of TMG$_2$dien was to generate a TBP high-spin oxoiron(IV) complex incorporating a labile site. To this end, adding (R_4N)N_3 or (R_4N)Cl to pre-formed solutions of **7** resulted in immediate UV−vis spectral changes (Figure 2 and Table 1). The new complexes, formulated as [Fe^{IV}(O)(TMG$_2$dien)(X)]$^+$ (**7-X**; X = N_3, Cl), exhibited spectra similar to those of the parent complex **7**. The presence of a terminal Fe=O unit in **7**, **7-N$_3$**, and **7-Cl** was confirmed by resonance Raman spectroscopy (Figure S3). The ν(Fe=O) vibrational modes were observed at 807, 833, and 810 cm^{-1}, respectively, and were downshifted upon ^{18}O labeling according to Hooke's Law (Table 1; theoretical $\Delta\nu \approx$ 36−37 cm^{-1}). Notably, **7-N$_3$** is of comparable stability to **7**, but **7-Cl** undergoes self-decay at a significantly accelerated rate ($t_{1/2}$ at −30 °C ≈ 34 and 2 min for **7-N$_3$** and **7-Cl**, respectively).

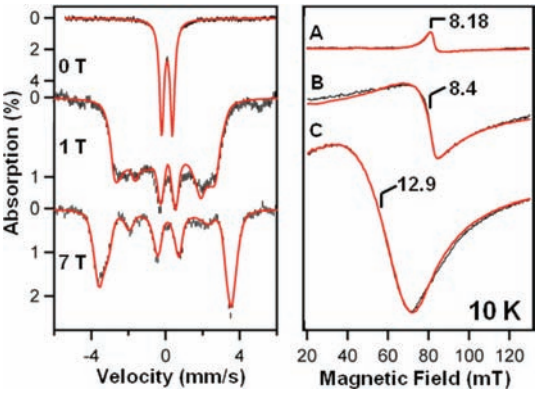

Figure 3. (left) Selected 4.2 K Mössbauer spectra of **7** in CH_3CN (black) recorded in parallel applied magnetic fields, as indicated. For all spectra, a high-spin Fe^{III} impurity representing ∼12% of the iron has been subtracted from the raw data. Solid red lines are spectral simulations using the parameters in Table 1. Additional spectra are shown in Figures S4−S7. (right) X-band EPR spectra (black) and spectral simulations using the parameters in Table 1 (red) for (A) **7-N$_3$**, (B) **7**, and (C) **7-Cl**. Additional spectra are shown in Figures S8−S10.

Mössbauer spectroscopy confirmed that complexes **7**, **7-N$_3$**, and **7-Cl** all contain $S = 2$ oxoiron(IV) centers (Figure 3 left and Figures S4−S7), with the zero-field spectrum of each exhibiting a doublet with an isomer shift of $\delta \approx 0.1$ mm s^{-1} (Table 1). Their distinct quadrupole splittings (ΔE_Q) confirmed the formation of new anion complexes. The three species were obtained in high yield, with **7**, **7-N$_3$**, and **7-Cl** accounting for 88, 80, and 87% (all ca. ±4%) of the Fe present, respectively. Minor iron(III) impurities accounted for the remainder. Fitting the Mössbauer spectra observed at variable applied fields B to an $S = 2$ spin Hamiltonian (see the SI) yielded zero-field splitting (D and E/D) and hyperfine parameters (Table 1) that compared well to those of other $S = 2$ oxoiron(IV) species.

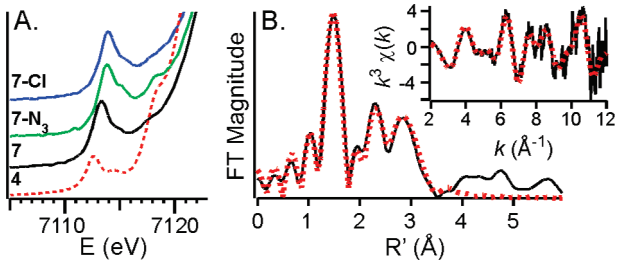

Figure 4. (A) XAS pre-edge region of **4** (red), **7** (black), **7-N$_3$** (green), and **7-Cl** (blue). (B) Fe K-edge unfiltered EXAFS data [inset: $k^3\chi(k)$] and the corresponding Fourier transform for **7-Cl**. The solid black lines and red dots correspond to the experimental data and fits, respectively. The fit of **7** and further details of the EXAFS analysis are provided in the SI.

The high-spin ground states of **7**, **7-N$_3$**, and **7-Cl** and the D and E/D values obtained by Mössbauer spectroscopy were confirmed by parallel-mode EPR spectroscopy (Figure 3 right and Figures S8−S10). Their X-band spectra all display broad resonances at $g \approx 8-13$ originating from the excited-state $M_S = \pm 2$ quasi-doublet of an $S = 2$ multiplet. As the intensity of such signals is proportional to E/D,[4] quantitative simulations allowed quite accurate determinations of E/D (Table 1; see Figures S8−S10 for further details).[11]

Consistent with their assignment as oxoiron(IV) complexes, **7**, **7-N$_3$**, and **7-Cl** exhibited X-ray absorption spectroscopy (XAS) edge energies $E_0 \approx 7124$ eV (Table 1), which are in the range observed for other oxoiron(IV) complexes and blue-shifted by ≥ 1.7 eV relative to the iron(II) starting material **4** ($E_0 = 7121.9$ eV). Unlike $S = 1$ oxoiron(IV) complexes, which exhibit a single symmetrical pre-edge feature,[12] **7**, **7-N$_3$**, and **7-Cl** all exhibited pre-edge features composed of two discernible peaks (Figure 4A and Table S3) originating from 1s → 3d electronic transitions. Consequently, two Gaussians were needed to model them successfully, as predicted by DFT for high-spin iron(IV) complexes.[13]

Analysis of the EXAFS data for both **7** and **7-Cl** furnished best fits (Tables S4 and S5, Figure 4B and Figure S11) with an O/N scatterer at ∼1.65 Å that corresponds to the Fe=O unit. (High-quality EXAFS data for **7-N$_3$** could not be obtained because of rapid photodecomposition.) These distances are comparable to the Fe=O lengths observed in the X-ray structures of **2** and **3** [1.661(2) and 1.680(1) Å, respectively],[5a,6] the EXAFS of enzymatic oxoiron(IV) intermediates,[2e,14b,15] and the plethora of existing $S = 1$ oxoiron(IV) complexes.[3,16] Both **7** and **7-Cl** also have a shell of O/N scatterers at ca. 1.94 Å (four in the former case and three in the latter) assigned to the N donors of the supporting ligands. This Fe−N distance is shorter than that found for **2** by EXAFS (1.99 Å),[5a] reflecting the lower steric constraints of the TMG$_2$dien ligand. Lastly, **7-Cl** has a Cl scatterer at 2.27 Å, a distance that is very similar to the 2.31 Å Fe−Cl distance obtained by EXAFS for the chloroferryl intermediate of the aliphatic halogenase SyrB2.[2e]

DFT calculations for **7**, **7-N$_3$** and **7-Cl** further supported our assignment of an $S = 2$ spin state for these three complexes (Tables S6−S13), all of which have a ^{5}A ground state with four d electrons located in two half-filled E levels (Table S7). The spin populations calculated for the iron and the oxo atoms were +3.0(1) and +0.6(1), respectively (Tables S9 and S10), similar to those obtained for **1**, **2**, and TauD-J.[4a,5a,14c] The geometry-optimized structures of **7**, **7-N$_3$**, and **7-Cl** (Figure 1C, Figure S12, and Table S8) are best described as TBP ($\tau = 0.79$, 0.83, and 0.72, respectively)[9] and have Fe=O bond lengths of ∼1.65 Å, in close agreement with EXAFS-derived distances. In contrast, the Fe−Cl distance of 2.35 Å calculated for **7-Cl** is somewhat longer than the value of 2.27 Å determined by EXAFS. Lastly, the DFT-calculated spin-dipolar contribution to the ^{57}Fe **A** tensor is in good agreement with the experimental data (Table S6), indicating that the z axis of the spin Hamiltonian (determined by the ZFS tensor) is oriented along the Fe−O bond (within ca. 5°).

Table 2. Second-Order Rate Constants (k_2) Observed in Reactions of Fe^{IV}=O Complexes with Various Substrates

	k_2 [M^{-1} s^{-1}][b]		
complex[a]	CHD	DHA	PPh$_3$
7	18	57	–[c]
2[d]	1.2	0.090	1.1
8[d]	1.3	2.0	1.5
9[d]	0.018	0.016	0.22
10[e]	94	310	–[c]

[a] [Fe^{IV}(O)(N4Py)]$^{2+}$ (**8**; N4Py = bis(2-pyridylmethyl)bis(2-pyridyl) methylamine), [Fe^{IV}(O)(TMC)(CH$_3$CN)]$^{2+}$ (**9**; TMC = 1,4,8,11-tetramethylcyclam), [Fe^{IV}(O)(Me$_3$NTB)]$^{2+}$ (**10**; Me$_3$NTB = tris((*N*-methylbenzimidazol-2-yl)methyl)amine). [b] Reactions were run in CH$_3$CN solution at −30 °C. The reaction kinetics for **2**, **8**, and **9** were measured using 1.0 mM complex. For **7**, the higher rates of reaction required the use of 0.1−0.2 mM complex and similarly reduced concentrations of the substrate. [c] This reaction was too fast for measurement of k_{obs}. [d] Reference 5a. [e] Obtained at −40 °C (see ref 17).

Besides the creation of an $S = 2$ oxoiron(IV) complex with a cis-labile site, it was anticipated that going from the tetradentate TMG$_3$tren ligand to the tridentate TMG$_2$dien ligand would provide substrates greater access to the Fe^{IV}=O unit, thereby allowing the inherent reactivity properties of the $S = 2$ oxoiron(IV) center to be manifested. Consistent with these expectations, the oxo-transfer reaction of **7** to PPh$_3$ proceeded so rapidly that we were unable to accurately measure the associated rate constants at −30 °C for comparison with published data for other oxoiron(IV) complexes listed in Table 2. Additionally, H-atom abstraction from 1,4-cyclohexadiene (CHD) and 9,10-dihydroanthracene (DHA), which are substrates with similarly weak C−H bonds but differing steric profiles, proceeded at comparable rates, with respective second-order rate constants that were 15 and 630 times larger than those for the more sterically hindered **2** (Table 2 and Figures S13−S15).

Notably, the reactivity of **7** was more than 1 and 3 orders of magnitude greater than those of the $S = 1$ complexes [Fe^{IV}(O)(N4Py)]$^{2+}$ (**8**) and [Fe^{IV}(O)(TMC)(CH$_3$CN)]$^{2+}$ (**9**), respectively (Table 2), which would appear to support DFT-based predictions of a more reactive $S = 2$ Fe^{IV}=O center.[7] However, **7** is an order of magnitude less reactive than the recently reported $S = 1$ complex [Fe^{IV}(O)(Me$_3$NTB)]$^{2+}$ (**10**).[17] This fact serves to highlight the difficulty of making such comparisons without consideration of the thermodynamic and steric consequences of the differing ligand environments of the various complexes. To date, there has been only one report of a pair of closely related complexes, namely, [(HO)(L)Fe$^{III/IV}$−O−Fe^{IV}(L)(O)] (L = tris(3,5-dimethyl-4-methoxypyridyl-2-methyl)amine), that have identical ligand environments but differ in having an

S = 1 or S = 2 oxoiron(IV) unit.[18] Remarkably, the high-spin $Fe^{III}Fe^{IV}$ complex was found to be 1000-fold more reactive than the low-spin $Fe^{IV}Fe^{IV}$ complex, thereby validating DFT-based predictions that an S = 2 Fe^{IV}═O center was superior to an S = 1 Fe^{IV}═O center at H-atom abstraction.[7]

In summary, we have described the synthesis of the high-spin oxoiron(IV) complex $[Fe^{IV}(O)(TMG_2dien)(CH_3CN)]^{2+}$ (**7**), which is related to the S = 2 complex $[Fe^{IV}(O)(TMG_3dien)(CH_3CN)]^{2+}$ (**2**) by replacement of one of the tetramethylguanidinyl arms of the TMG_3tren ligand by a methyl group and inclusion of a solvent ligand in its place. This modification provides greater access to the Fe^{IV}═O subunit, eliminating the selectivity for smaller substrates exhibited by **2** and resulting in a significant increase in the rates of intermolecular reactions. Furthermore, the introduction of CH_3CN as an equatorial ligand in **7** provides a means to access a series of anion-substituted S = 2 oxoiron(IV) complexes that are highly amenable to characterization, as illustrated here for $[Fe^{IV}(O)(TMG_2dien)(X)]^{+}$ (**7-X**; X = N_3, Cl). This offers the promise of elucidating spectroscopic and reactivity trends as a function of the electronic properties of an S = 2 oxoiron(IV) center and may provide answers to specific biorelevant questions, such as the reason for the omnipresence of carboxylato ligands in non-heme enzymes[1] and the cause of the inherent preference for halogen- versus oxygen-atom rebound in non-heme iron halogenases.[19]

■ ASSOCIATED CONTENT

Supporting Information. Experimental and synthetic details; resonance Raman spectra; additional X-ray crystallographic, Mössbauer, EPR, XAS, DFT, and kinetics information; and CIF files. This material is available free of charge via the Internet at http://pubs.acs.org.

■ AUTHOR INFORMATION

Corresponding Author
eb7g@andrew.cmu.edu; emunck@cmu.edu; larryque@umn.edu

■ ACKNOWLEDGMENT

This work was supported by the NIH (Grants GM33162 to L.Q. and EB001475 to E.M. and postdoctoral fellowships ES017390 to M.A.C. and GM093479 to K.M.V.H.) and the NSF (Grants CHE1058248 to L.Q. and CHE070073 to E.L.B. through Teragrid resources provided by NCSA). XAS data were collected at Beamline 7-3 of the Stanford Synchrotron Radiation Lightsource. The SSRL Structural Molecular Biology Program is supported by the DOE Office of Biological and Environmental Research and by the NIH National Center for Research Resources Biomedical Technology Program (P41RR001209). Data collection and structure solution were conducted by Victor G. Young, Jr., at the X-ray Crystallographic Laboratory, Department of Chemistry, University of Minnesota.

■ REFERENCES

(1) (a) Krebs, C.; Galonić Fujimori, D.; Walsh, C. T.; Bollinger, J. M., Jr. *Acc. Chem. Res.* **2007**, *40*, 484. (b) Kovaleva, E. G.; Lipscomb, J. D. *Nat. Chem. Biol.* **2008**, *4*, 186.

(2) (a) Eser, B. E.; Barr, E. W.; Frantom, P. A.; Saleh, L.; Bollinger, J. M., Jr.; Krebs, C.; Fitzpatrick, P. F. *J. Am. Chem. Soc.* **2007**, *129*, 11334. (b) Price, J. C.; Barr, E. W.; Tirupati, B.; Bollinger, J. M., Jr.; Krebs, C. *Biochemistry* **2003**, *42*, 7497. (c) Hoffart, L. M.; Barr, E. W.; Guyer, R. B.; Bollinger, J. M., Jr.; Krebs, C. *Proc. Natl. Acad. Sci. U.S.A.* **2006**, *103*, 14738. (d) Galonić, D. P.; Barr, E. W.; Walsh, C. T.; Bollinger, J. M., Jr.; Krebs, C. *Nat. Chem. Biol.* **2007**, *3*, 113. (e) Matthews, M. L.; Krest, C. M.; Barr, E. W.; Vaillancourt, F. H.; Walsh, C. T.; Green, M. T.; Krebs, C.; Bollinger, J. M., Jr. *Biochemistry* **2009**, *48*, 4331.

(3) Que, L., Jr. *Acc. Chem. Res.* **2007**, *40*, 493.

(4) Pestovsky, O.; Stoian, S.; Bominaar, E. L.; Shan, X.; Münck, E.; Que, L., Jr.; Bakac, A. *Angew. Chem., Int. Ed.* **2005**, *44*, 6871.

(5) (a) England, J.; Martinho, M.; Farquhar, E. R.; Frisch, J. R.; Bominaar, E. L.; Münck, E.; Que, L., Jr. *Angew. Chem., Int. Ed.* **2009**, *48*, 3622. (b) England, J.; Guo, Y.; Farquhar, E. R.; Young, V. G., Jr.; Münck, E.; Que, L., Jr. *J. Am. Chem. Soc.* **2010**, *132*, 8635.

(6) Lacy, D. C.; Gupta, R.; Stone, K. L.; Greaves, J.; Ziller, J. W.; Hendrich, M. P.; Borovik, A. S. *J. Am. Chem. Soc.* **2010**, *132*, 12188.

(7) (a) Ye, S.; Neese, F. *Curr. Opin. Chem. Biol.* **2009**, *13*, 89. (b) Decker, A.; Rohde, J.-U.; Klinker, E. J.; Wong, S. D.; Que, L., Jr.; Solomon, E. I. *J. Am. Chem. Soc.* **2007**, *129*, 15983. (c) Bernasconi, L.; Louwerse, M. J.; Baerends, E. J. *Eur. J. Inorg. Chem.* **2007**, 3023. (d) Hirao, H.; Kumar, D.; Que, L., Jr.; Shaik, S. *J. Am. Chem. Soc.* **2006**, *128*, 8590.

(8) (a) Janardanan, D.; Wang, Y.; Schyman, P.; Que, L., Jr.; Shaik, S. *Angew. Chem., Int. Ed.* **2010**, *49*, 3342. (b) Wong, S. D.; Bell, C. B., III; Liu, L. V.; Kwak, Y.; England, J.; Zhao, J.; Que, L., Jr.; Solomon, E. I. *Angew. Chem., Int. Ed.* **2011**, *50*, 3215.

(9) Addison, A. W.; Rao, T. N.; Reedijk, J.; Van Rijn, J.; Verschoor, G. C. *J. Chem. Soc., Dalton Trans.* **1984**, 1349.

(10) Macikenas, D.; Skrzypczak-Jankun, E.; Protasiewicz, J. D. *J. Am. Chem. Soc.* **1999**, *121*, 7164.

(11) Surerus, K. K.; Hendrich, M. P.; Christie, P. D.; Rottgardt, D.; Orme-Johnson, W. H.; Münck, E. *J. Am. Chem. Soc.* **1992**, *114*, 8579.

(12) (a) Jackson, T. A.; Rohde, J.-U.; Seo, M. S.; Sastri, C. V.; DeHont, R.; Stubna, A.; Ohta, T.; Kitagawa, T.; Münck, E.; Nam, W.; Que, L., Jr. *J. Am. Chem. Soc.* **2008**, *130*, 12394. (b) Rohde, J.-U.; Torelli, S.; Shan, X.; Lim, M. H.; Klinker, E. J.; Kaizer, J.; Chen, K.; Nam, W.; Que, L., Jr. *J. Am. Chem. Soc.* **2004**, *126*, 16750.

(13) Berry, J. F.; DeBeer George, S.; Neese, F. *Phys. Chem. Chem. Phys.* **2008**, *10*, 4361.

(14) (a) Proshlyakov, D. A.; Henshaw, T. F.; Monterosso, G. R.; Ryle, M. J.; Hausinger, R. P. *J. Am. Chem. Soc.* **2004**, *126*, 1022. (b) Riggs-Gelasco, P. J.; Price, J. C.; Guyer, R. B.; Brehm, J. H.; Barr, E. W.; Bollinger, J. M., Jr.; Krebs, C. *J. Am. Chem. Soc.* **2004**, *126*, 8108. (c) Sinnecker, S.; Svensen, N.; Barr, E. W.; Ye, S.; Bollinger, J. M., Jr.; Neese, F.; Krebs, C. *J. Am. Chem. Soc.* **2007**, *129*, 6168.

(15) Fujimori, D. G.; Barr, E. W.; Matthews, M. L.; Koch, G. M.; Yonce, J. R.; Walsh, C. T.; Bollinger, J. M., Jr.; Krebs, C.; Riggs-Gelasco, P. J. *J. Am. Chem. Soc.* **2007**, *129*, 13408.

(16) (a) Rohde, J.-U.; In, J.-H.; Lim, M. H.; Brennessel, W. W.; Bukowski, M. R.; Stubna, A.; Münck, E.; Nam, W.; Que, L., Jr. *Science* **2003**, *299*, 1037. (b) Klinker, E. J.; Kaizer, J.; Brennessel, W. W.; Woodrum, N. L.; Cramer, C. J.; Que, L., Jr. *Angew. Chem., Int. Ed.* **2005**, *44*, 3690. (c) Thibon, A.; England, J.; Martinho, M.; Young, V. G., Jr.; Frisch, J. R.; Guillot, R.; Girerd, J.-J.; Münck, E.; Que, L., Jr.; Banse, F. *Angew. Chem., Int. Ed.* **2008**, *47*, 7064.

(17) Seo, M. S.; Kim, N. H.; Cho, K.-B.; So, J. E.; Park, S. K.; Clémancey, M.; Garcia-Serres, R.; Latour, J.-M.; Shaik, S.; Nam, W. *Chem. Sci.* **2011**, *2*, 1039.

(18) Xue, G.; De Hont, R.; Münck, E.; Que, L., Jr. *Nat. Chem.* **2010**, *2*, 400.

(19) (a) Matthews, M. L.; Neumann, C. S.; Miles, L. A.; Grove, T. L.; Booker, S. J.; Krebs, C.; Walsh, C. T.; Bollinger, J. M., Jr. *Proc. Natl. Acad. Sci. U.S.A.* **2009**, *106*, 17723. (b) de Visser, S. P.; Latifi, R. *J. Phys. Chem. B* **2009**, *113*, 12. (c) Kulik, H. J.; Blasiak, L. C.; Marzari, N.; Drennan, C. L. *J. Am. Chem. Soc.* **2009**, *131*, 14426. (d) Borowski, T.; Noack, H.; Radoń, M.; Zych, K.; Siegbahn, P. E. M. *J. Am. Chem. Soc.* **2010**, *132*, 12887. (e) Pandian, S.; Vincent, M. A.; Hillier, I. H.; Burton, N. A. *Dalton Trans.* **2009**, 6201.